

Abstract

The couplings between Higgs and the second generation of quarks are sensitive to some BSM models, which predict that the couplings between Higgs and charm/strange quarks are larger than they are in the SM. A search for SM Higgs boson decaying to a J/ψ and a photon, with subsequent decay of the J/ψ to $\mu^+\mu^-$ is presented. The analysis is performed using data recorded by CMS detector from pp collision at center-of-mass energy of 13 TeV corresponding to an integrated luminosity of 36.42 fb^{-1} . We put a limit on $H \rightarrow J/\psi + \gamma$ decay branching fraction at 9.17×10^{-4} , which is about 327 times the SM prediction.

Introduction

The process $H \rightarrow J/\psi + \gamma$, with the subsequent decay $J/\psi \rightarrow \mu^+\mu^-$, is a promising but challenging channel in studying the Higgs-Charm coupling at LHC [1, 2]. The continuum decay of the Higgs with the same final state occurring through the loop diagram, $H \rightarrow \gamma^* \gamma \rightarrow \mu\mu\gamma$, referred to as Higgs Dalitz decay, is considered as a part of background and is subtracted when deriving the limit.

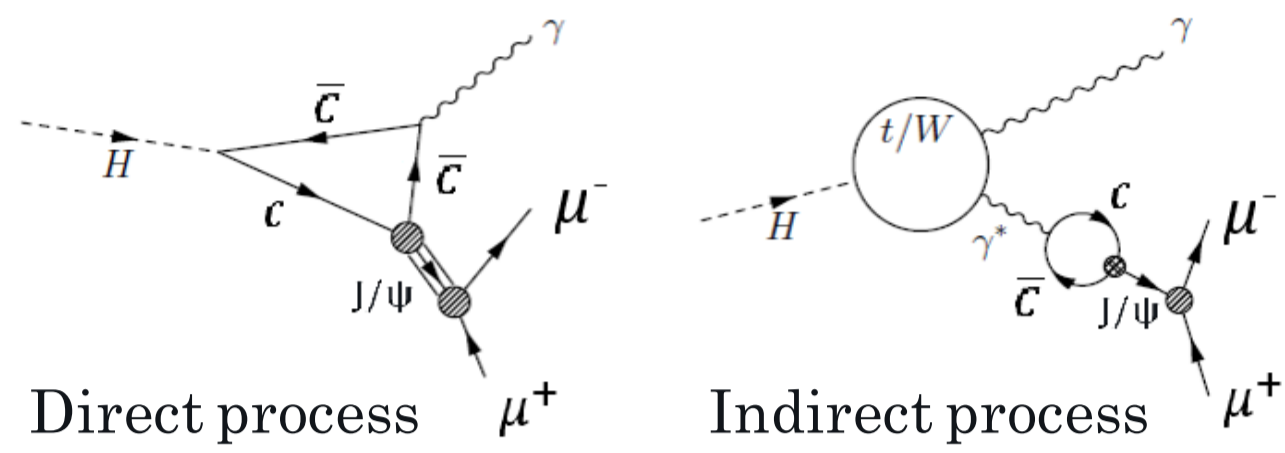


Fig. 1: The Feynman diagrams of $H \rightarrow (J/\psi)\gamma \rightarrow \mu\mu\gamma$ decay

Advantage	Disadvantage
• Very clean event signature	• Large QCD background
• Low background condition	• in the hadron collider
• Good mass resolution	• Rare decay

Table 1: The advantage and disadvantage of $H \rightarrow (J/\psi)\gamma \rightarrow \mu\mu\gamma$ channel [3]

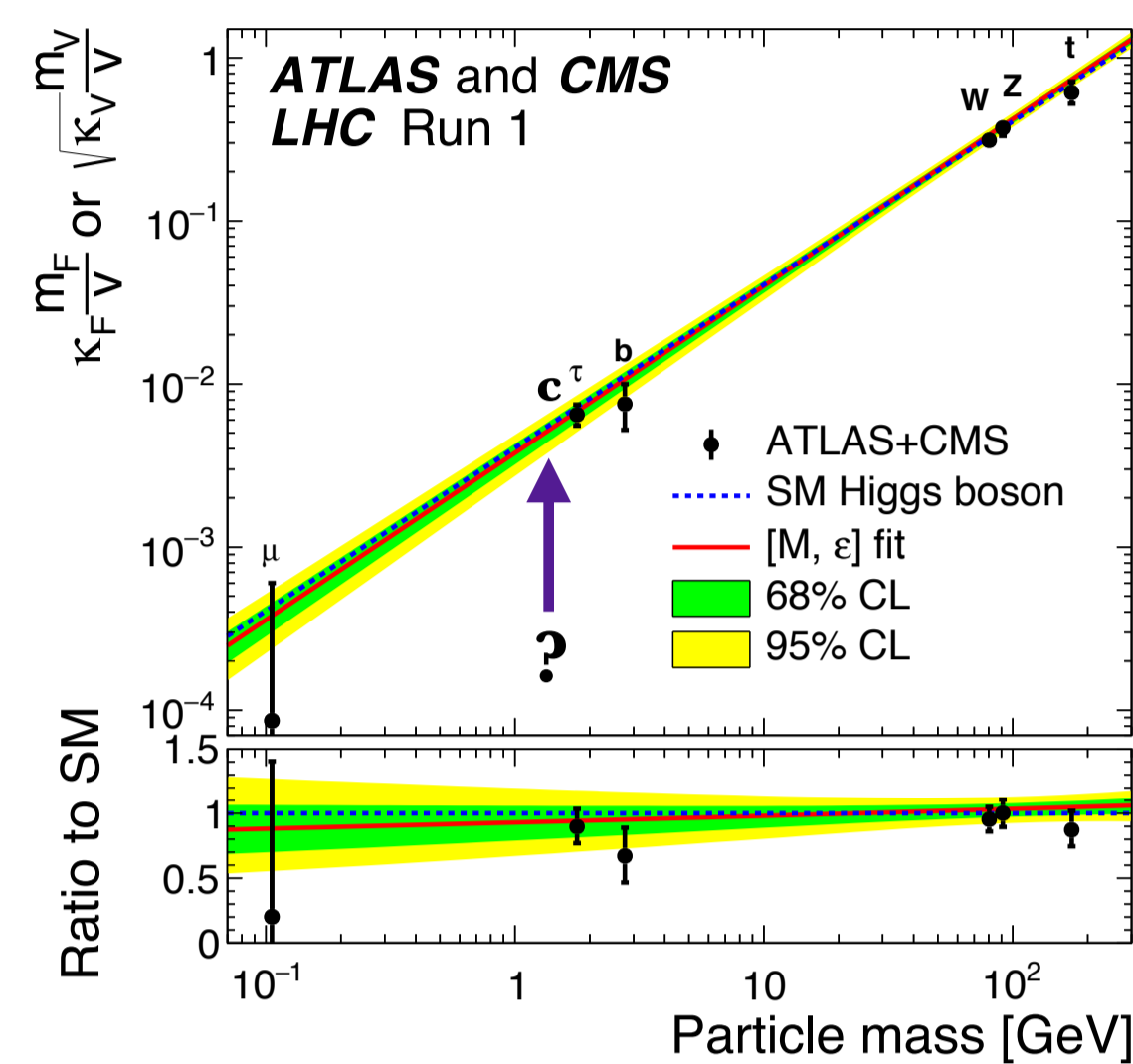
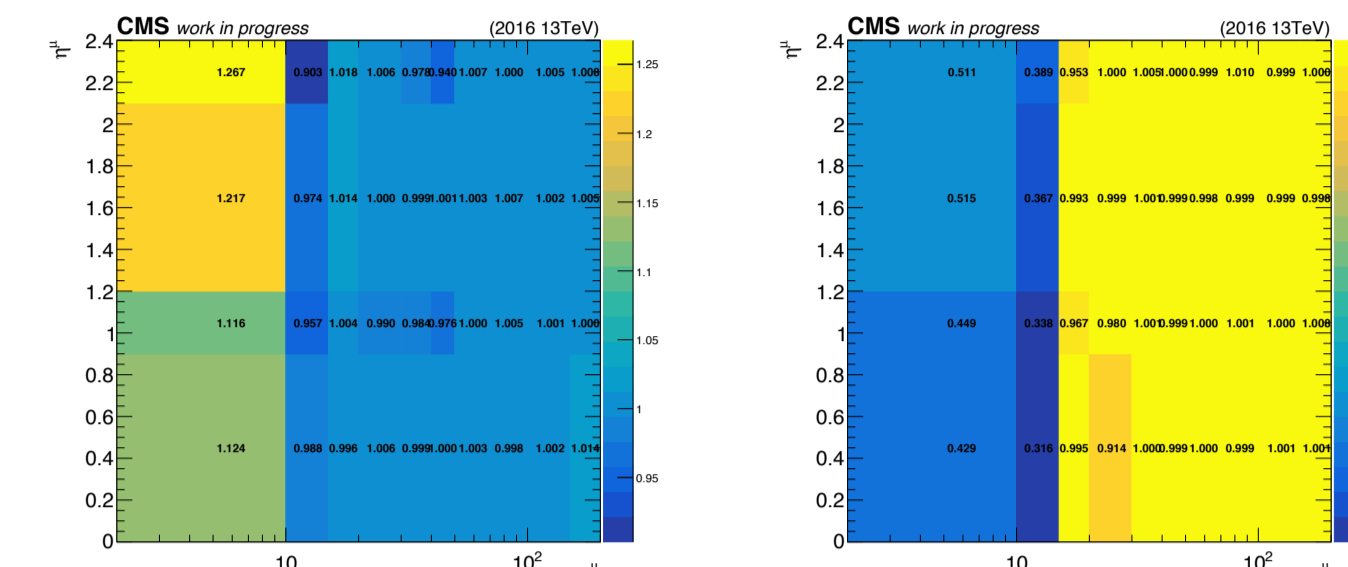


Fig. 2: The couplings of Higgs and other particles [4].

Muon ID/Isolation & $\mu\text{-}\gamma$ trigger efficiency

Since this analysis uses non-standard Loose Muon ID, the scale factors for both Muon ID and Isolation are derived independently using tag-and-probe method.



$$\text{SFs for } \begin{cases} p_T < 15 \text{ GeV} \\ p_T > 15 \text{ GeV} \end{cases} \begin{cases} \text{Use } J/\psi \rightarrow \mu\mu \text{ events} \\ \text{Use } Z \rightarrow \mu\mu \text{ events} \end{cases}$$

Fig. 6: Scale factors for Muon ID (left) and Isolation (right)

The trigger efficiency is measured using $Z \rightarrow \mu\mu\gamma$ events in Single muon datasets and is applied to MC as a global factor.

	Tag	Probe
Object	muon	muon+photon
Requirement	<ul style="list-style-type: none"> • Fire the single muon trigger • Tight muon ID • Isolation 	<ul style="list-style-type: none"> • $H \rightarrow J/\psi\gamma$ offline selection • Kinematic cuts are used to select pure $Z \rightarrow \mu\mu\gamma$ events

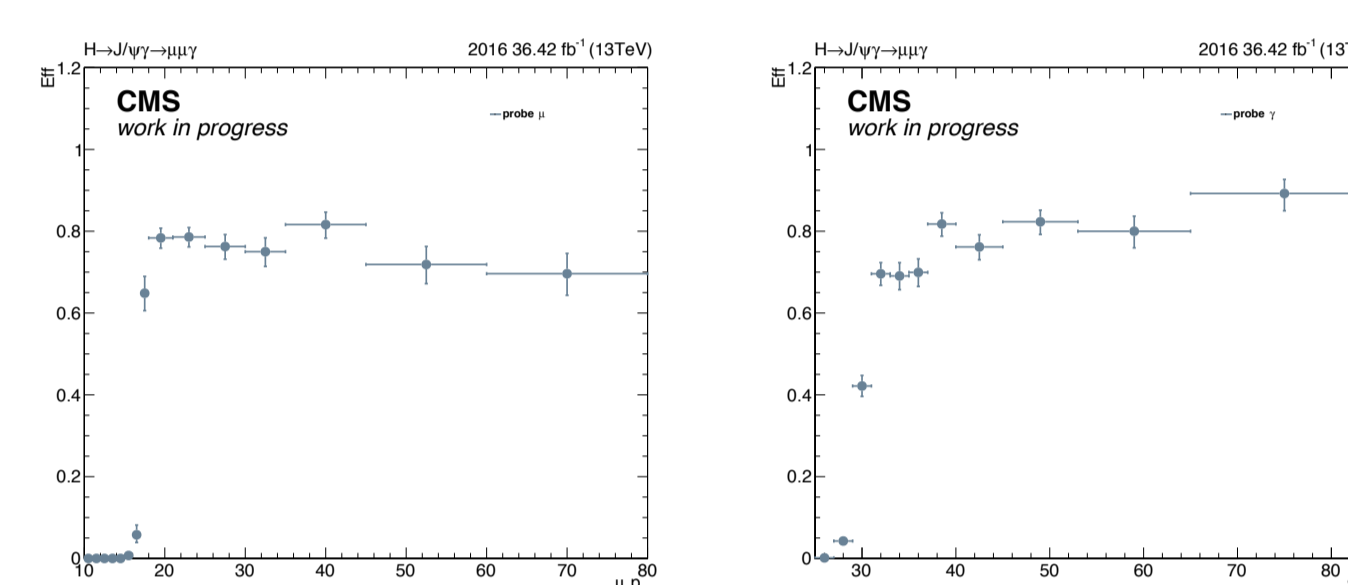


Fig. 7: ϵ^{Trig} as function of p_T^μ (left) and E_T^{photon} (right)

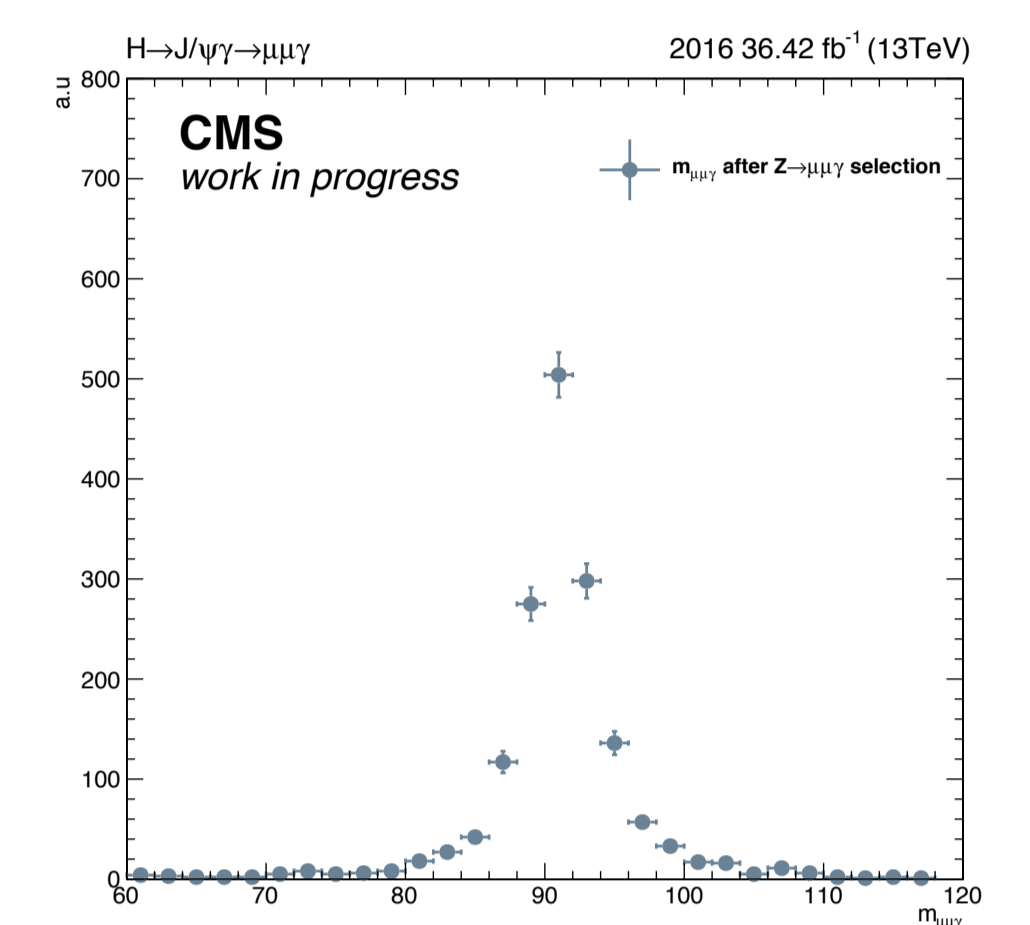
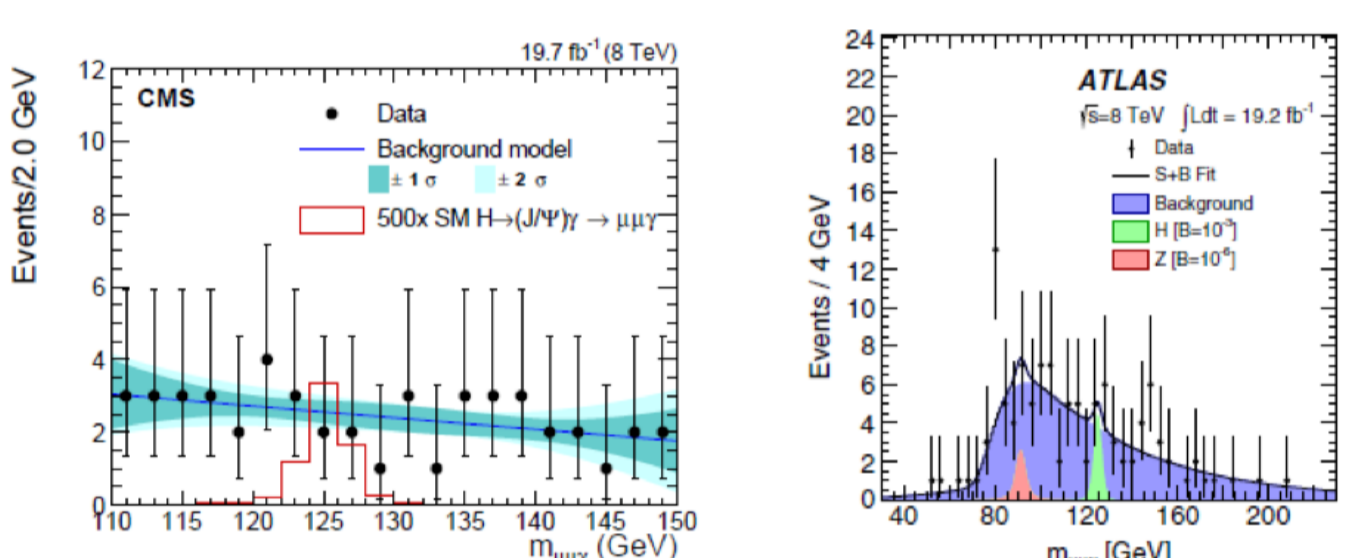


Fig. 8: $m_{\mu\mu}$ distribution after $Z \rightarrow \mu\mu\gamma$ selection

Previous results from CMS and ATLAS

The search for the process $H \rightarrow (J/\psi)\gamma$ has been performed in CMS and ATLAS with $\sqrt{s}=8\text{ TeV}$ pp collision. Both show that no significant excess of events is observed above the background.



95% C.L. upper limits		
	ATLAS	CMS
Expected	1.2×10^{-3}	1.2×10^{-3}
Observed	1.5×10^{-3}	1.5×10^{-3}

Fig. 3: The left plot is the result of CMS [5], while the middle one is of ATLAS [6]. The right table shows the expected and observed branching fraction limits at 95% C.L. for $\sqrt{s}=8\text{ TeV}$.

Event selection & Event yields

Table 2 below summarizes the baseline selection criteria in the analysis.

1	Trigger	Muon-Photon trigger with $p_T^\mu > 17\text{ GeV}$ and $E_T^{\text{photon}} > 30\text{ GeV}$
2	Muon selection	Official Loose ID, muons must originate from the primary vertex $p_T^{\text{lead } \mu} > 20\text{ GeV}$; $p_T^{\text{trail } \mu} > 4\text{ GeV}$; $ \eta^\mu < 2.4$; Isolation is applied on μ^{lead}
3	Photon selection	Photon MVA ID; $ \eta_{\text{SC}}^{\text{photon}} < 2.5$ (exclude those in ECal gap region); $\Delta R(\mu, \gamma) > 1$
4		$2.95 < m_{\mu\mu} < 3.25\text{ GeV}$, $110 < m_{\mu\mu\gamma} < 150\text{ GeV}$, $p_T^{\text{mu}}/m_{\mu\mu\gamma} > 0.28$, $E_T^{\text{photon}}/m_{\mu\mu\gamma} > 0.28$

Table 2: Selection criteria

Category	Selection criteria	Data	$H \rightarrow J/\psi\gamma$ signal	$H \rightarrow \gamma^*\gamma$ background
	Total (Before selection)	170M	0.335	76.7
	After full selection	288	0.0796	0.382
Expected yields (with the pile-up weight, all the scale factors and efficiencies)				
	$ \eta_{\text{SC}}^{\text{photon}} < 1.4442$ (Cat1)	201	0.0623	0.302
	$1.566 < \eta_{\text{SC}}^{\text{photon}} < 2.5$ (Cat2)	87	0.0173	0.080

Table 3: Observed and expected yields after full selection

Fig. 4. shows the di-muon mass distribution after full selection in both categories.

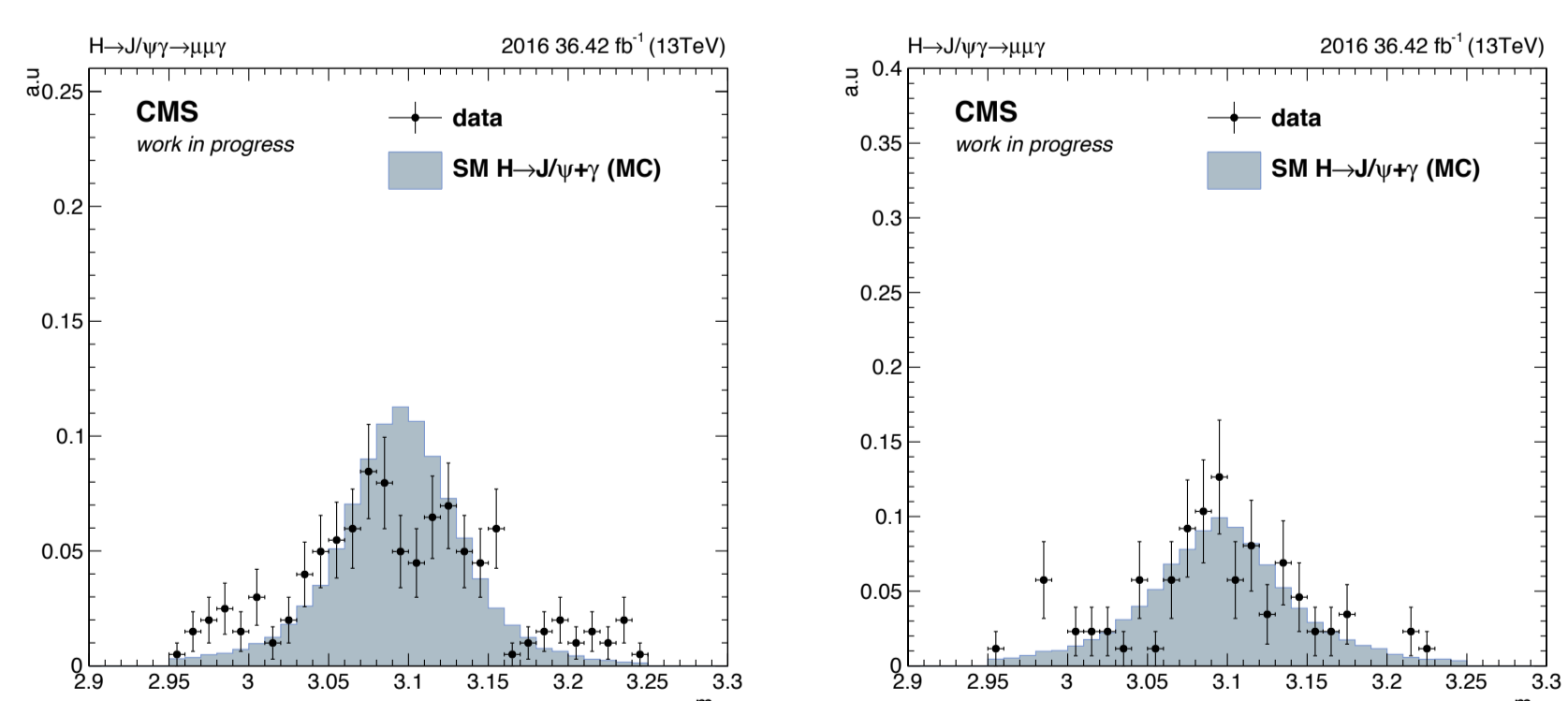


Fig. 4: The di-muon mass distribution in Cat1 (left) and Cat2 (right).

The fit to reconstructed $m_{\mu\mu\gamma}$ with Bernstein 2nd order polynomial over the range $110 < m_{\mu\mu\gamma} < 150\text{ GeV}$ is used as background model. The signal shape is modeled using Gaussian plus a Crystal-Ball function with the same mean. The $m_{\mu\mu\gamma}$ distributions in Cat1 and Cat2 are shown in Fig. 5.

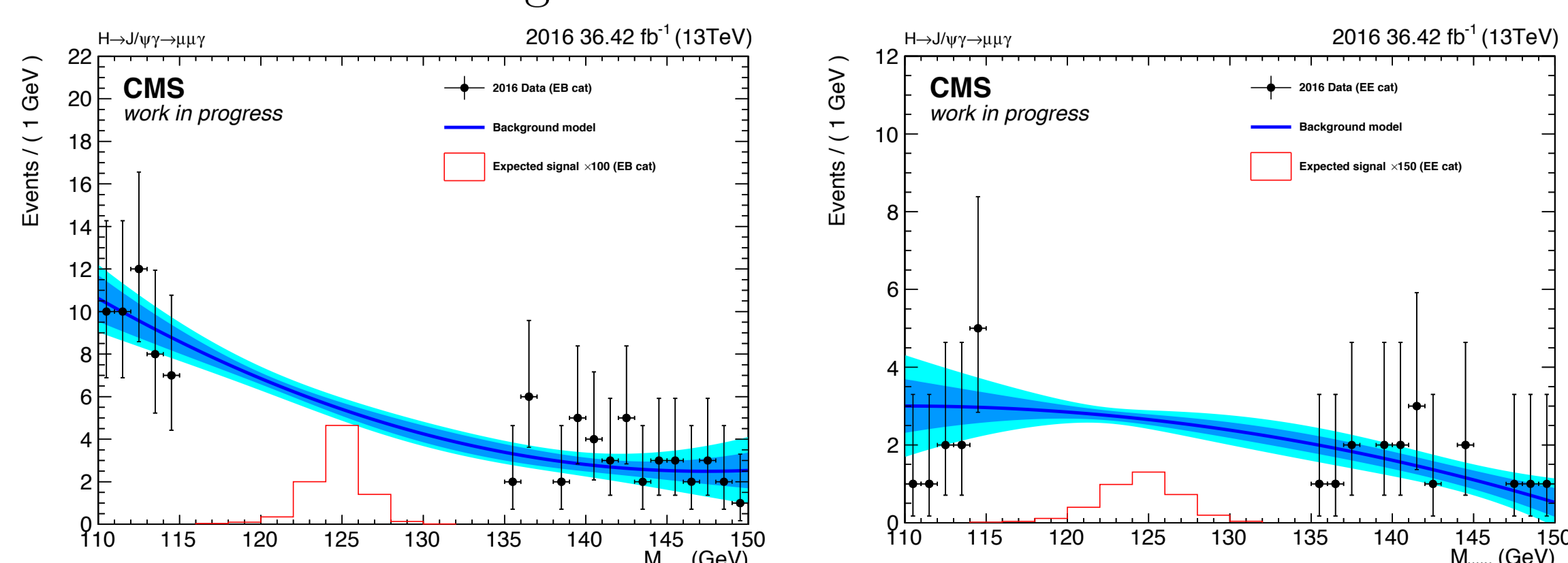


Fig. 5: The $m_{\mu\mu\gamma}$ distributions in Cat1 (left) and Cat2 (right).

Systematic uncertainty

Table 3 shows the full list of systematic uncertainties used in this analysis. A procedure to ensure that the fits are unbiased is performed. The pull distributions of $(\mu_{\text{Sig(Fit)}} - \mu_{\text{Sig(True)}})/\sigma_{\text{Sig(Fit)}}$ obtained in different combinations of true and fit functions are fitted with Gaussian, and the mean values are used to identify if the function used is unbiased. We use Bernstein 2nd order polynomial as background shapes for both Cat1 and Cat2.

Source	Uncertainty	
	Category	
	Cat1	Cat2
Integrated luminosity	6.2%	
Theoretical uncertainties		
SM Higgs production cross section (scale)	3.0%	
SM Higgs production cross section (PDF + α_s)	7.0%	
SM Higgs Dalitz decay branching fraction	10.0%	
Detector simulation, reconstruction:		
Pileup reweighting	1.0%	1.0%
Trigger (per event)	10.0%	
Muon ID	1.0%	
Muon Isolation	0.5%	
Photon MVA ID Scale factors	0.8%	0.8%
Electron veto Scale factors	1.1%	1.1%
Signal model fits:		
Mean(scale)	0.26%	0.25%
Sigma(resolution)	3.8%	1.6%

Table 3: List of systematic uncertainties

Current results & Outlook

The expected upper limit at 95% Confidence Level is set:

$$\sigma(\text{pp} \rightarrow H) \times \text{BR}(H \rightarrow (J/\psi)\gamma \rightarrow \mu\mu\gamma) < 3.01\text{ fb}$$

with 1σ band:

$$2.11 < \sigma \times B < 4.36\text{ fb}$$

The $\sigma(\text{pp} \rightarrow H) = 55.6\text{ pb}$ and the $\text{BR}(J/\psi \rightarrow \mu\mu) = 0.059$, we can derive the limit on $\text{BR}(H \rightarrow (J/\psi)\gamma)$:

$$\text{BR}(H \rightarrow (J/\psi)\gamma) < 9.17 \times 10^{-4}$$

which is about 327 times the SM prediction.

In the Run-2, LHC is expected to collect 300 fb^{-1} of data at $\sqrt{s}=13\text{ TeV}$. It's expected to increase the sensitivity of $H \rightarrow (J/\psi)\gamma \rightarrow \mu\mu\gamma$ about a factor of 3.

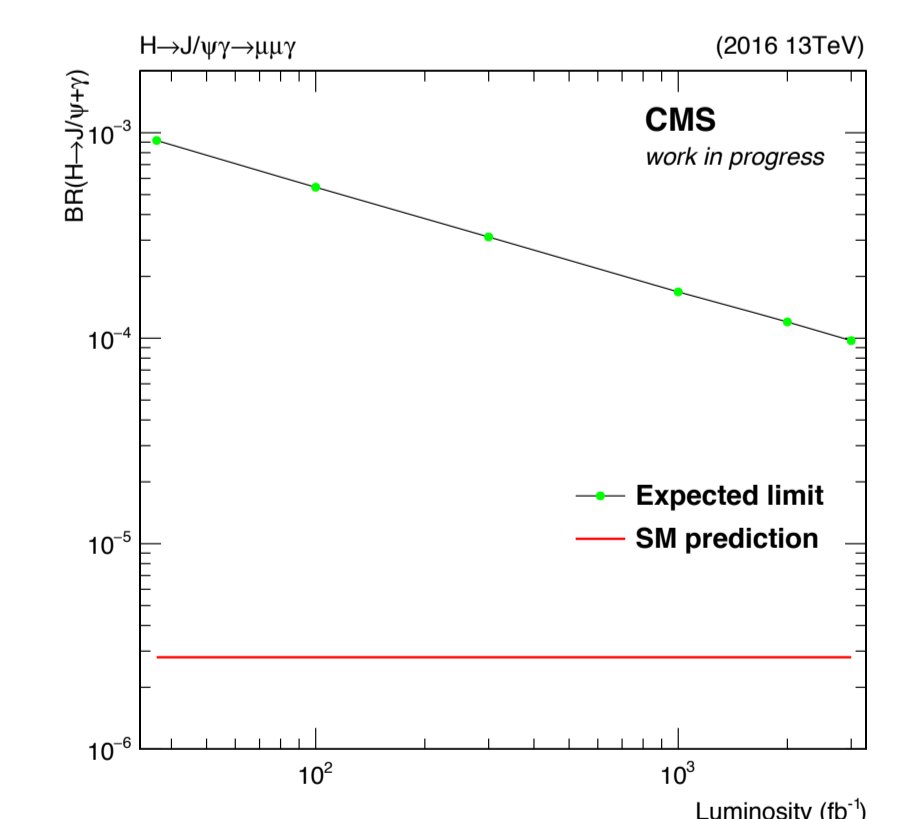


Fig. 9: The expected limit on $\text{BR}(H \rightarrow (J/\psi)\gamma)$

Summary

- The preliminary results on $H \rightarrow (J/\psi)\gamma$ search at 13 TeV is performed with 2016 36.42 fb^{-1} data. The limit on the branching ratio of this decay is approximately 327 times SM prediction, while in Run1 it's 540 times SM value.

Reference

- [1] A. Pozdnyakov, S. Stoynev, M. Velasco et al., CMS AN 2013/335 (2013).
- [2] G. T. Bodwin, F. Petriello, Brian Pollack et al, Phys. Rev. D88 (2013) 053003.
- [3] G. T. Bodwin et al., Phys. Rev. D 90, 113010 (2014)
- [4] ATLAS, CMS Collaborations, JHEP08(2016)045
- [5] CMS Collaboration, Physics Letters B 753 (2016) 341–362
- [6] ATLAS Collaboration, Phys. Rev. Lett. 114 (2015) 121801